Published in final edited form as:
Biomaterials. 2012 March ; 33(7): 2197–2205. doi:10.1016/j.biomaterials.2011.11.063.

Activation of Inflammasomes by Tumor Cell Death Mediated by Gold Nanoshells

Hai T. Nguyen, **Kenny K. Tran**, **Bingbing Sun**, and **Hong Shen***
Department of Chemical Engineering, University of Washington, Box 351750, Seattle, WA 98195, USA

Abstract

Gold nanoshell enabled photothermal therapy (NEPTT) utilizes the efficient thermal conversion of near infrared (NIR) light for the ablation of cancer cells. Cancer therapies that combine cell killing with the induction of a strong immune response against the dying tumor cells have been shown to increase therapeutic efficacy in the clearance and regression of cancers. In this study, we assessed the ability of dying cells generated by *in vitro* NEPTT to activate inflammasome complexes. We quantified levels of major danger-associated molecular patterns (DAMPs), including adenosine triphosphate (ATP), adenosine diphosphate (ADP), and uric acid, released from tumor cells treated by NEPTT. The amount of DAMPs released was dependent on the dose of nanoshells internalized by cells. However, under all the employed conditions, the levels of generated DAMPs were insufficient to activate inflammasome complexes and to induce the production of pro-inflammatory cytokines (i.e. IL-1β). The results from this study provide insights into the development of nanoplasmonics for combining both photothermal therapy and immunotherapy to eradicate cancers.

Keywords

gold nanoshell; nanoplamonics; apoptosis; necrosis; NALP3 inflammasome; DAMPs; immunotherapy

1. Introduction

Significant progress in the development of nanoplasmonics with the high efficiency of energy conversion from near-infrared light (NIR) to heat has instigated recent advances in photothermal therapy for cancer treatment [1]. Gold nanoshell/silica cores represent one of the promising platforms and their efficacy has been demonstrated both *in vitro* and *in vivo* [2–4]. We termed the photothermal therapy based on gold nanoshells as gold nanoshell-enabled photothermal therapy (NEPTT) in this study.

One of the key roles of the immune system is to clear dying cells in the body and generate the appropriate response to the dying cells or their cellular components. Programmed cell death or apoptosis of cells is generally considered not to elicit inflammation or an immune response, which would otherwise result in autoimmunity. Cell death can lead to an immunogenic response when they undergo specific forms of necrosis or stress that result in

*Corresponding author. Tel.: +1 206 543 5961. hs24@u.washington.edu (H. Shen).

the preservation and release of various danger-associated molecular patterns (DAMPs) [5]. Photothermally induced cell damage can occur either by apoptosis or necrosis depending on the laser dosage, type, irradiation time, and the subcellular distribution of nanoplasmonics [4, 6–8]. It has been reported that NEPTT induces necrotic cell death [4, 6, 7].

The immune system recognizes DAMPs through a series of receptors either on the surface or within the cytoplasm of cells. Some of the toll-like receptors (TLRs) that mainly recognize pathogen-associated molecular patterns (PAMPs), have been shown to detect DAMPs. TLR2 and 4 recognize high mobility group box 1(HMGB1) protein[9], hyaluronan [10], biglycan [11], and heat shock proteins (HSPs) [12]. The stimulation of TLR2 and 4 can induce the production of pro-IL-1β and pro-IL-18 that can be cleaved into the active secreted form by the caspase-1 complex associated with the activation of inflammasome complexes [13].

Another group of receptors implicated in sensing cell death and injury are the NOD-like receptors (NLRs). Some NLRs, such as NLRP1, NLRC4, and AIM2 inflammasome, primarily involve pathogen recognition [13]. The NALP3 inflammasome has been shown to be activated by a wide range of pathogen associated danger signals as well as DAMPs. The DAMPs that can activate the NALP3 inflammasome include extracellular ATP [14], ADP, AMP [15], uric acid and monosodium urate (MSU) crystals [16]. Uric acid released from dying cells has been shown to crystallize into MSU in the extracellular environment due to the presence of high levels of sodium ions [17, 18]. Iyer and colleagues also suggest that actively-respiring mitochondria that are released from necrotic cells can activate the NALP3 inflammasome possibly through the generation of ATP [19].

Inflammasomes form high molecular weight complexes that lead to the activation of caspase-1 to cleave precursors of proinflammatory cytokines, such as IL-1β and IL-18 [13]. The generation of IL-1β, a potent proinflammatory cytokine, is believed to be the key mediator in the generation of a cascade of immune responses [20]. It can recruit neutrophils to the site of injury [21], promote the maturation of dendritic cells (DCs) [22], contribute to priming of $CD8^+$ T-cells [22], induce the differentiation of type 17 T-helper cells [23], and stimulate the production of various downstream molecules such as nitric oxide (NO) and proinflammatory cytokines such as IL-6 [24] and IL-12[25]. Activation of the inflammasome complexes has been shown to be required for the development of adaptive immune responses against tumors [22].

Recently, cancer therapies that combine cell killing by various modalities such as chemotherapy with the induction of a strong immune response against dying tumor cells have been shown to increase therapeutic efficacy in the clearance and regression of cancers [22]. The induction of immune responses to tumor cells during combined therapies involves the generation of DAMPs by the treatments and the stimulation of the innate immune sensors by DAMPs, followed by the recognition and presentation of tumor associated antigens (TAAs) to T cells by antigen presenting cells (i.e. DCs) for the establishment of TAA-specific immune responses [22].

Towards the goal of eradicating and preventing the recurrence of tumors, an important question for the development of nanoplasmonics remains to be addressed: does NEPTT simply perform a microsurgery, which only removes the tumor mass, or can it also mobilize immune responses against tumors? In this study, we confirmed that NEPTT by continuous wave (cw) NIR laser induced necrotic cell death. Subsequently, we assessed whether DAMPs released from NEPTT-treated cells stimulated inflammasome complexes and whether they were able to activate macrophages for the generation of proinflammatory

cytokines, i.e. IL-1β. Our results provide critical insights into the development of nanoplasmonics for combining photothermal therapy and immunotherapy to treat cancers.

2. Materials and Methods

2.1. Materials

Tetraethyl orthosilicate, ammonia, (3-Aminopropyl) trimethoxysilane, gold (III) chloride hydrate, sodium bicarbonate, tetrakis(hydroxymethyl)phosphonium chloride solution, sodium chloride, and sodium carbonate were obtained from Sigma-Aldrich (St. Louis, MO) and used as received. Carbon monoxide gas was obtained from Praxair (Danbury, CT). Cell culture supplies were obtained from Invitrogen (Carlsbad, CA). Min-U-Sil-15 was kindly provided by U.S. Silica (Berkeley Springs, WV). Adenosine 5′-triphosphate (ATP) disodium salt hydrate was obtained from Invivogen (San Diego, CA). Enzyme-linked immunosorbent assay (ELISA) reagents were obtained from eBiosciences (San Diego, CA)

2.2. Cell Culture

TC-1 cells (ATCC) were maintained in Roswell Park Memorial Institute (RPMI) 1640 media supplemented with 10% fetal bovine serum (FBS), 2 mM L-glutamine, 1 mM sodium pyruvate, 10 mM (4-(2-hydroxyethyl)-1-piperazineethanesulfonic acid)(HEPES), 1.5 g/L sodium bicarbonate and 4.5 g/L glucose. 9L gliosarcoma rat cells (ATCC), B16 melanoma (ATCC), and J774A.1 mouse macrophage cells (ATCC) were maintained in Dulbecco's Modified Eagle medium (DMEM) containing 10% fetal bovine serum (FBS), 1% Penicillin-Streptomycin, 4 mM L-glutamine, and 1 mM sodium pyruvate at 37°C and 5% CO_2. Hela cells (ATCC) were maintained in MEM media supplemented with 10% FBS, 1% Penicillin-Streptomycin, 2 mM L-glutamine, and 1 mM sodium pyruvate at 37°C and 5% CO_2. THP-1 cells were maintained in RPMI 1640 supplemented with 10% FBS, 2 mM L-glutamine, 1 mM sodium pyruvate, 10 mM HEPES, 50 μM 2-mercaptoethanol, 1.5 g/L glucose. All the cells were maintained at 37 °C and 5% CO_2.

2.3. Synthesis of Au Nanoshells

The method employed to synthesize the gold nanoshell/silica core particles was adapted from Oldenburg *et al* [26] and Brinson *et al* [27]. In brief, silica cores with a mean diameter of 110 nm were prepared using the Stober process [28]. 1.5 ml tetraethyl orthosilicate (TEOS) was added drop-wise to a 50 ml ethanol solution containing 3.2 ml 70% ammonia, resulting in condensation reactions self-nucleating into monodisperse particles. They were subsequently functionalized with 25 μl (3-Aminopropyl)trimethoxysilane (APTMS) overnight followed by gentle boiling for one hour to enhance attachment. The particles were washed 3 times by centrifugation, and redispersed in 50 ml of absolute ethanol. 2–3 nm colloidal gold particles were prepared using a method originally described by Duff *et al* [29]. 2 ml 1% gold chloride solution was added to a 45ml solution of water containing 0.5 ml NaOH and 12 μl of the reducing agent tetrakis(hydroxymethyl)phosphonium chloride (THPC), and quickly reacted to form the colloidal gold particles as indicated by the development of a dark reddish brown hue. The synthesized colloidal gold particles were attached to the surface of the silica nanoparticles through electrostatic interactions by adding 0.5 ml of the functionalized silica particles to 4 ml of excess colloidal gold solution followed by purification through centrifugation and wash cycles before being redispersed in 5 ml Milli-Q deionized water. The colloidal gold on the surface acted as nucleation sites for further reduction of gold ions onto silica core.

The nanoshell reducing solution was prepared by adding 25 mg of potassium carbonate to 100 ml of Milli-Q deionized water. After 10 min of stirring, 1.5 ml of a 1% gold chloride solution was added to the reduction solution. The solution was then aged overnight at 4°C

prior to use. The nanoshells formed were concentrated through centrifugation and redispersed in Milli-Q deionized water prior to use. Gaseous carbon monoxide, the reducing agent, was bubbled at 25 ml/min into a mixture of 4 ml of the gold reducing solution and between 100–200 μl of the colloidal gold coated silica particles. The completion of the gold reduction was indicated by the development of blue shade in the reaction mixture.

2.4. Characterization of Au Nanoshells

The bare and gold nanoshell-coated silica particles were characterized by scanning electron microscopy (SEM) (JOEL 7200 SEM) and UV-Vis spectroscopy (Molecular Devices Spectramax M5). The particle size was calculated based on SEM images. The shell thickness was estimated based on the images of bare silica and gold nanoshell-coated silica particles. The size distribution and aggregation of nanoshells were examined by the dynamic light scattering using a Malvern Zetasizer Nano ZS (Malvern Instruments Ltd Worcestershire, UK).

The silica particle concentration was calculated based on the average volume of each individual silica particle and the total silica volume for a given amount of TEOS. The molecular weight and density of the silica particles was assumed to be similar to bulk values. Gold nanoshell/silica core nanoparticle concentration was estimated based on the quantity of silica particles assuming no loss of silica particles during the growth of gold nanoshells. For convenience, the term Au nanoshells, was used in the text to represent gold nanoshell/silica core nanoparticles.

2.5. NEPTT

TC-1, B16, and J774A.1 cells at 6×10^4 cells/well were plated in flat bottom 24 well plates and allowed to adhere for 24 h. Au nanoshells were collected by centrifugation and re-dispersed in FBS-free cell culture media, and diluted to the designated concentrations. Cells were incubated with 500 μl of Au nanoshell solutions for 4 h. Cells were then rinsed with Dulbecco's phosphate-buffered saline (DPBS) three times to remove unbound Au nanoshells prior to the laser irradiation. Hela cells were plated at 3×10^4 cells/well in flat bottom 96 well plates incubated with 100 μl of Au nanoshell solutions for 4 h. Cells were imaged under a bright-field microscope (Nikon Eclipse TE2000-U) with a CCD camera (Photometrics Coolsnap ES) to confirm Au nanoshell internalization. Images were taken at the same exposure level and magnification for all samples.

Cells were detached with 0.05% trypsin-EDTA and re-suspended in 100 μl of DPBS. Cells were irradiated in a well of 96-well plate using a diode laser (Newport Corporation, 808 nm, 23 W/cm^2 max), which was positioned to illuminate the full area of the well of the 96-well plate. Immediately following the irradiation, the temperature of the solution in the well was measured. The cells obtained from two wells were combined for further analysis and the stimulation of macrophages.

Other means of inducing necrosis, including the incubation of cells in a 70°C water bath (water bath) for 5 min, and 3 cycles of freeze-thaw (freeze-thaw), were used as controls.

2.6. Analysis of Cell Death by Flow Cytometry

The apoptosis assay kit (Annexin V, BD Biosciences) was used for the assessment of cell viability and mode of cell death using flow cytometry. The laser-irradiated cells and controls were washed 2 times with cold phosphate buffered saline (PBS) and then re-suspended in the binding buffer. Cells were stained with 5 μl each of the Annexin V-FITC and 7-AAD dyes and incubated for 15 min prior to FACS analysis. The samples were analyzed within one hour using a BD FACScan (Cell Analysis Facility, University of Washington).

Apoptotic cells were positive for the Annexin V-FITC dye, while the necrotic cells were positive for both the Annexin V-FITC and 7-AAD. Viable cells were negative for both dyes.

2.7. Stimulation of macrophages

J774A.1 cells were initially primed in 24 well plates with 2 μg/ml lipopolysaccharide (LPS) from Escherichia coli 0111:B4 (Sigma) for 24 h. THP-1 cells were first differentiated into macrophages using 500 nM phorbol-12-myristate-13-acetate (PMA) for 6 hours, followed by priming with 2 μg/ml LPS for 8 hours. The primed J774A.1 and THP-1 cells were washed once with DPBS followed by the culture media. Then they were stimulated with fractions of cells subjected to NEPTT, 2 mM ATP in DPBS, or 1 mg/ml Min-U-Sil 15 silica crystals in DPBS. J774A.1 cells and THP-1 cells with and without LPS priming were stimulated with cell culture media containing DPBS as negative controls to determine the background level of IL-1β. LPS primed macrophages were stimulated with 0–2 mM ATP, 0–10 mM ADP, and 0–100 μM MSU crystals to determine the concentration required to activate the inflammasome complex for those DAMPs.

2.8. ATP Quantification

ATP levels released from NEPTT-treated and untreated cells were quantified using a Promega Enliten ATP assay (Promega Corp.). The samples were diluted serially up to the concentration range suitable for the assay. Luciferase enzyme solution was mixed quickly with diluted samples at a 1:1 ratio in an opaque white Costar 96-well plate with low background luminescence. The luminescence was measured by a Spectramax M5 plate reader. Luminescence from all wavelengths was collected over a 1000 ms-integration time. At least three separate measurements at each dilution within the assay range were taken. The concentration of each sample was determined by averaging the values obtained from three dilutions.

2.9. ADP Quantification

ADP levels released from NEPTT-treated and untreated cells were quantified using a Transcreener ADP^2 FI Assay (Bellbrook Labs). Samples were diluted serially up to the concentration range suitable for the assay. ADP^2 Antibody-IRDye QC-1 was mixed with diluted samples at 1:1 ratio to a final volume of 50 μl and a final dye concentration of 4 nM in an opaque black 96-well plate. The fluorescence intensity was measured by a Spectramax M5 plate reader with an excitation wavelength of 590 nm and an emission wavelength of 617 nm.

2.10. Uric Acid Quantification

Levels of uric acid in the supernatants from NEPTT- and un- treated cells were quantified using both the uricase enzyme and the Ampliflu Red peroxidase reagent (Sigma-Aldrich) using a protocol based on the method used by Gasse and colleagues [30]. Uricase converts the uric acid into allantoin, hydrogen peroxide, and carbon dioxide. Hydrogen peroxide in the presence of horseradish peroxidase (HRP) reacts with the Ampliflu Red reagent to produce the fluorescent product resorufin. Supernatants were diluted two times in 0.1 ml Tris-HCl and mixed with an equal part of a reaction solution containing 100 μM Amplifu Red reagent, 0.4 U/ml HRP, and 0.4 U/ml uricase. Fluorescence intensity was measured by a Spectramax M5 plate reader with an excitation wavelength of 540 nm and an emission wavelength of 590 nm.

2.11. Enzyme-linked Immunosorbent Assay (ELISA)

The level of IL-1β secreted by macrophages was assessed by ELISA. For the J774A.1 IL-1β quantification, anti-mouse/rat IL-1β was used as the capture antibody (clone B122) and

biotinylated polyclonal rabbit anti-mouse IL-1β antibody (polyclonal) was used as the detection antibody. For THP-1 IL-1β quantification, anti-human IL-1β (clone CRM56) was used as the capture antibody and biotinylated mouse anti-human IL-1β antibody (clone CRM57) was used as the detection antibody. Samples were diluted at a proper range with blocking buffer (1% FBS/PBS). The detection range for IL-1β was 8-2000 pg/ml. Standard procedures described in eBioscience protocol literature (eBioscience San Diego, CA) were used.

2.12. Statistical analysis

All results are representative of at least two sets of independent experiments, with samples performed in duplicates or triplicates. Results represent average values with error bars representing ± the standard deviation (SD) of the samples.

3. Results

3.1. Characterization of gold nanoshell/silica core nanoparticles (Au nanoshells)

Au nanoshells consist of a silica core 119 ± 11nm in diameter (Figure 1a) and a 17 nm gold shell (Figure 1b). The shell thickness was determined by comparing bare silica and Au nanoshells (Figure 1a, b). Au nanoshells exhibited little aggregation in aqueous solutions and had a polydispersity index of 0.28. The Au nanoshells exhibited a broad absorption with a surface plasmon resonance peak at 780 nm (Figure 1c). The ability of Au nanoshells to convert light energy into heat was tested by using water as the heating medium. The water containing Au nanoshells displayed a marked temperature increase within 1 minute upon the laser irradiation (Figure 1d). These results confirmed that the Au nanoshells used in this study exhibited similar dimensions, optical and thermal properties as used in previous studies [2, 3, 26].

3.2. Cellular uptake of Au nanoshells

Initially, we confirmed the cellular uptake of Au nanoshells by both microscopic analysis and a semi-quantitative method (Figure 2). By using a light microscope, we observed that the cellular uptake of Au nanoshells increased as the concentration of Au nanoshells that cells were exposed to increased. It is difficult to determine whether Au nanoshells were endocytosed inside cells or simply associated with the surface of cells. The fluorescence signals of fluorescent molecules are quenched when they are near the surface of gold nanoparticles [31]. Based on this observation, we developed a semi-quantitative method to measure the intracellular level of Au nanoshells by flow cytometry. The fluorescent molecule calcein at a fixed concentration was codelivered to cells along with different doses of Au nanoshells. Calcein has been shown to be internalized into endosomal compartments [32, 33]. The fluorescent intensity of calcein, quantified as mean fluorescent intensity (MFI), was linearly reduced as the dose of Au nanoshells cells were exposed to increased (Figure 2b), confirming microscopic observations (Figure 2a). However, the flow cytometry method was not able to quantify the number of Au nanoshells internalized per cell and was not sensitive enough to determine the uptake when the dose of nanoshells decreased to 20,000 nanoshells/cell.

3.3. Cell death induced by NEPTT

Subsequently, we assessed the cell death induced by irradiating Au nanoshell-loaded cells using near infrared light with a wavelength of 810 nm (Figure 3). Above the dose of 25,000 Au nanoshells/cell, nearly 100% of cells underwent necrotic cell death. As the dose of Au nanoshells decreased, cells mainly underwent necrotic cell death though the fraction of viable cells increased. Either Au nanoshells (Control) or laser irradiation alone (Control +

Laser) caused negligible cell death. Our results are consistent with previous studies when non-targeted nanoshells and cw laser were used[4]. As previously reported, cells subjected to high temperature(>50°C) or freeze-thaw underwent necrotic cell death [19, 34, 35]. The end temperature of cell suspensions was monitored after NEPTT treatment. The end temperature linearly increased from 37°C to 70°C when the dose of Au nanoshells increased from 5,000 to 100,000 Au nanoshells/cell. The minimum temperature at which complete necrotic cell death occurred by NEPTT treatment was 50°C.

3.4. Stimulation of inflammasome complexes by cellular components released from NEPTT-treated cells

Recent studies suggest that cellular components released from dead cells caused by chemotherapeutic drugs [22], pressure-disruption, or complement-mediated lysis stimulate inflammasomes but not cells killed by UV irradiation or freeze-thaw cycles [19, 22]. We examined whether cellular components from NEPTT-treated cells would trigger inflammasomes. In this study, a mouse macrophage cell line, J774A.1, and a human macrophage cell line, THP-1, were used. THP-1 and J774A.1 have been well characterized as cell lines that respond to a variety of well-documented inflammasome-inducers [36, 37]. J774A.1 and THP-1 cells were first treated with lipopolysaccharide (LPS) to induce pro-IL-1β. Upon the stimulation of inflammasomes, pro-IL-1β is cleaved into IL-1β which is secreted from cells. The stimulation of inflammasomes was therefore characterized by the secretion of IL-1β in J774A.1 and THP-1 cells.

B16 cells loaded with various doses of Au nanoshells were irradiated and separated into secreted, nuclear and mitochondrial fractions. Initially, all the fractions were tested for the activation of inflammasomes. None of the fractions induced IL-1β secretions in both macrophage cell lines (data not shown). Subsequently, only secreted fractions were used to test the effect of Au nanoshell concentrations and the ratio of dead cells to macrophages. Regardless of the concentrations of Au nanoshells, secreted fractions from dead cells did not induce a significantly higher level of IL-1β in macrophages compared to untreated cells (Figure 4a). Higher ratios of dead cells to macrophages did not activate inflammasomes either (Figure 4b). Macrophages in the absence of LPS pre-treatment also did not generate IL-1β. In order to confirm our results from B16 tumor cells, a number of other tumor cell lines derived from either mouse or human tissues were tested for their ability of stimulating inflammasomes. None of these cell lines activated the inflammasome complexes to produce IL-1β (Figure 5).

3.5. Quantification of ATP, ADP and monosodium urate (MSU) released from NEPTT-treated cells

We next quantified the levels of major DAMPs, including ATP, ADP and MSU that have been suggested to be responsible for the stimulation of inflammasomes by necrotic cells [15, 19, 38]. The level of ATP released from NEPTT-treated cells is about 0.004 mM or less than 20 fmoles/cell (Supplementary Table 1) and significantly higher than untreated cells ($p < 0.05$) (Figure 6a). However, concentrations greater than 1 mM ATP were required to activate inflammasomes and induce IL-1β secretion alone (Figure 6b). Iyer and colleagues [15]have suggested respiring mitochondria released from pressure-disrupted or complement induced-lysis of cells actively produce ATP that is responsible for inflammasome activation [19]. They have also shown that heating to 65°C inactivated the mitochondria and reduced the ATP level released from cells as well as the inflammasome activation. Tong and colleagues have observed that Au nanorod-enabled laser irradiation damages mitochondria [8]. The temperatures at which necrotic cell death was induced by NEPTT were often greater than 60°C (Figure 3) [4]. As a result, NEPTT may have destroyed the respiring

mitochondria and reduced the level of ATP generated. It is also possible that the mitochondria were not released upon cell death as hypothesized by Iyer and colleagues [19].

ATP-mediated inflammasome activation occurs through activation of the $P2X_7$ receptor found on many immune cells [14]. Exonucleases on the surface of the cell membrane or in the extracellular milieu may degrade ATP [18]. The degradation products of ATP, including ADP and AMP, have not been shown to directly activate the inflammasome, but their ability to activate $P2X_7$ receptors and induce IL-1β secretion has been suggested [15]. ADP, the product of ATP de-phosphorylation by ATPases, was quantified for both its presence in the secreted components of NEPTT cells (Figure 6c) and its ability to induce inflammasome activation (Figure 6d). ADP levels generated by cells treated with NEPTT were higher than untreated cells, but more than 100 times below the threshold required to produce significant levels of IL-1β. We did not quantify AMP due to the lack of agents specific for AMP.

Uric acid, a product of purine metabolism, is released by dying cells into the extracellular environment and has been found to activate inflammasome complexes. The immunostimulatory effects of uric acid occur at the supersaturation condition (>70 μg/ml (~417μM)), indicating that MSU crystal formation is required [16, 39]. Uric acid released following NEPTT was present at insufficient levels to activate inflammasome complexes (Figure 6e-f). This was likely due to the low uric acid levels generated by NEPTT-treated cells, which was insufficient to induce the formation of MSU crystals.

In summary, higher levels of ATP, ADP, and uric acid were detected from NEPTT-treated cells compared to untreated-cells, indicating that DAMPs were released from NEPTT-treated cells following cell death and membrane disruption. However, the levels of these DAMPs were not sufficient to activate inflammasome complexes.

4. Discussion

The hidden self model proposes that endogenous DAMPs are located within the interior of the cell, and are only released following membrane disruption and release of the cytosolic components [5]. We have demonstrated that NEPTT-treated cells underwent necrosis and their cell membrane became permeable (Figure 3). However, the NEPTT-treated cells were poor in stimulating inflammasome complexes and proinflammatory cytokine secretions (Figure 4 and 5). The inability to stimulate inflammasomes was due to insufficient levels of the inflammasome-associated DAMPs generated (Figure 6). Levels of ATP released from NEPTT-treated cells were 3–4, ADP was 2–3, and uric acid was 1–2 orders of magnitude lower than required to activate the inflammasomes. Uric acid concentrations were not sufficient to precipitate into MSU crystals, but even the presence of MSU crystals at the concentration of uric acid found in the supernatant was not sufficient to activate the inflammasome complexes.

We recognize that *in vitro* cell culture systems can be different from what could occur *in vivo* or in clinical settings. We estimated the possible level of major DAMPs released from a tumor mass 5 mm in radius and containing 5×10^6 cells (Supplementary Table 1). We assumed that all the cells were loaded with sufficient levels of Au nanoshells and underwent necrotic death after NEPTT treatment. Two extreme scenarios were considered: one was that DAMPs were confined within the tumor volume, and another was that DAMPs were immediately diluted into blood. NEPTT-treated cells could trigger inflammasome complexes in the first scenario but not for the second scenario. The first scenario, however, unlikely occurs since many DAMPs are small molecules and tend to diffuse away from local tumor sites. Some DAMPs are prone to be degraded and lose their activity (such as ATP). Additionally, it is nearly impossible to load all cells within a tumor mass, especially cells

located in the interior of the tumor, with a sufficient level of Au nanoshells as observed previously [40].

NEPTT-treated cells may be immunogenic through non-inflammasome pathways. A number of other DAMPs associated with necrotic cell death have been identified, including heat shock proteins (HSPs) [41], high mobility group box 1(HMGB1) protein [42], S100 proteins [43], DNA [44], RNA [45], and the cytokine IL-6 [46].

HSPs, including HSP70, HSP90, and GP96, are expressed in cells in response to thermal stress [35, 47]. These HSPs are immunogenic and can be recognized by CD14, CD40, CD91, TLR2, or TLR4 [51, 52]. They activate a variety of signaling pathways that induce proinflammatory cytokines (i.e. TNF-α, IL-1β, IL-6, IL-2) and play a role in DC maturation and antigen presentation [5, 12]. The up-regulation of HSPs is generally associated with mild to moderate heating at sub-lethal doses. The release of HSPs and subsequent immune response are generally associated with necrotic cell death [48]. Thermal ablation of cells that results in drastic temperature increase and coagulative necrosis may not allow for sufficient levels of HSP expression prior to cell death. Radiofrequency ablation used to generate temperatures in the range of 65°C to 123°C within a tumor showed little to no HSP70 within the tumor core but high HSP70 generation in the tumor periphery where the temperature was significantly lower [49, 50]. Thermal ablation with multi-walled carbon nanotube-enabled NIR photothermal therapy showed similar results for HSP27, HSP70, and HSP90: high temperatures within the tumor corresponds to areas with little to no HSPs, and low temperatures in the periphery of tumor corresponds to high levels of HSPs. The temperatures generated during NEPTT are greater than 60°C where coagulative necrosis would occur [4]. Therefore, it is unlikely that significant levels of HSPs could be generated prior to cell death.

HMGB1, a nuclear protein that is secreted from necrotic cells, acts upon a number of receptors including TLR2, TLR4, and the receptor for advance glycation end products (RAGE). The activation of these receptors involves the MyD88/NF-κB signaling pathways and upregulates pro-IL-1β [5, 9]. HMGB1 has been shown to translocate from the nucleus and subsequently released into the lysate following heating at 43.7°C, 47°C and 56°C [50]. The level of HMGB1 increases as the temperature increases up to 56°C. Under NEPTT conditions, HMGB1 could be induced. We did not directly measure HMGB1 and the production of pro-IL-1β. We tested the production of IL-1β in absence of LPS priming. The level of IL-1β was negligible. NEPTT might induce little or no HMGB1. Even if significant levels of HMGB1 were produced, other DAMPs would be required to activate the inflammasome complex to cleave pro- IL-1β into its active secreted form.

Other immunostimulatory cellular constituents such as DNA, RNA, S100 proteins, and IL-6 have also been associated with necrotic cell death [5, 51]. Low levels of DNA and RNA were released from NEPTT-treated cells (data not shown). Proteins and enzymes are likely to be inactivated during NEPTT or unable to be expressed before the cell death due to the rapid and drastic temperature increase [52].

DNA and RNA, and HSPs from necrotic cells are able to induce the maturation of DCs and up-regulate surface molecules, such as CD86 and MHC II [44, 45, 53]. We did examine whether B16 cells treated with NEPTT were able to activate immature DCs at different Au nanoshell dosages and the ratio of B16 to DCs (Supplementary Figure 1). The up-regulation of both CD86 and MHCII on immature DCs were negligible compared to untreated cells. These results further confirm that NEPTT-treated cells did not release a significant level of HSPs, DNA and RNA.

Taken together, cell death induced by NEPTT by cw laser irradiation displays weak immunogenicity. The effect of a non-immunogenic form of cell death on the efficacy of the therapy can have a range of consequences. The lack of an innate immune response may simply decrease the ability of DCs to become activated, mature, and process and present antigens, failing to establish effective adaptive immune responses against the tumor cells. Therefore, complete eradication of tumors will only rely on the primary photothermal therapy. A potential negative consequence may be the induction of immune tolerance to the tumor cells. Liu and colleagues found that mice developed a tolerogenic response to cell-associated antigen delivered in dying cells that possibly did not produce significant levels of DAMPs [54]. A tolerogenic response can result in a poor prognosis due to recurrence of tumors.

We recognize that the generation of DAMPs from necrotic cells is modality-dependent. In this study, we used Au nanoshells as the model system and studied the activation of inflammasomes complexes and immature DCs. These results can be extended to other nanoplasmonics, such as gold nanorods, which have similar mechanisms of photothermal effects. cw laser was used in this study. NEPTT has also been performed by nanosecond laser pulses. It requires additional investigations on whether sufficient levels of DAMPs can be generated by laser pulses. In this study, Au nanoshells were internalized and distributed throughout cytoplasm. Au nanoshells or other nanoplasmonics have been targeted to either cell membrane or subcellular compartments. It is possible that targeting membrane can induce necrotic cell death while permitting the generation, preservation and release of sufficient levels of DAMPs.

5. Conclusion

Laser irradiation mediated by nanoplasmonics, including Au nanoshells, represents a promising means of surgical removal of tumors through thermal treatment. Thermal injury by NEPTT did not result in significant levels of DAMPs to activate the inflammasome complexes and induce proinflammatory cytokines, such as Il-1β. The lack of activation of inflammasomes and maybe other receptors for DAMPs potentially suppress the generation of adaptive immune responses to the tumor following NEPTT. The results from this study give insights into the development of nanoplasmonics for combined photothermal therapy and immunotherapy of cancers.

Supplementary Material

Refer to Web version on PubMed Central for supplementary material.

Acknowledgments

The authors would like to thank Dr. Liguo Wang for reviewing the manuscript. This study was funded by the NSF Career Award to H.S., AI088597 from the National Institute of Allergy and Infectious Diseases (NIAID) and the Office of Research on Women's Health (ORWH) and University of Washington. The content is solely the responsibility of the authors and does not necessarily represent the official views of NIAID, ORWH or NIH.

References

1. Huang X, Jain PK, El-Sayed IH, El-Sayed MA. Plasmonic photothermal therapy (PPTT) using gold nanoparticles. Lasers Med Sci. 2008; 23:217–28. [PubMed: 17674122]
2. Hirsch LR, Stafford RJ, Bankson JA, Sershen SR, Rivera B, Price RE, et al. Nanoshell-mediated near-infrared thermal therapy of tumors under magnetic resonance guidance. Proc Natl Acad Sci U S A. 2003; 100:13549–54. [PubMed: 14597719]

3. O'Neal DP, Hirsch LR, Halas NJ, Payne JD, West JL. Photo-thermal tumor ablation in mice using near infrared-absorbing nanoparticles. Cancer Lett. 2004; 209:171–6. [PubMed: 15159019]
4. Stern JM, Stanfield J, Kabbani W, Hsieh JT, Cadeddu JRA. Selective prostate cancer thermal ablation with laser activated gold nanoshells. J Urol. 2008; 179:748–53. [PubMed: 18082199]
5. Chen GY, Nunez G. Sterile inflammation: sensing and reacting to damage. Nat Rev Immunol. 2010; 10:826–37. [PubMed: 21088683]
6. Tong L, Zhao Y, Huff TB, Hansen MN, Wei A, Cheng JX. Gold nanorods mediate tumor cell death by compromising membrane integrity. Adv Mater. 2007; 19:3136–41. [PubMed: 19020672]
7. Huang XH, Kang B, Qian W, Mackey MA, Chen PC, Oyelere AK, et al. Comparative study of photothermolysis of cancer cells with nuclear-targeted or cytoplasm-targeted gold nanospheres: continuous wave or pulsed lasers. J Biomed Opt. 2010; 15:058002-1–7. [PubMed: 21054128]
8. Tong L, Cheng JX. Gold nanorod-mediated photothermolysis induces apoptosis of macrophages via damage of mitochondria. Nanomedicine. 2009; 4:265–76. [PubMed: 19331536]
9. Yu M, Wang HC, Ding AH, Golenbock DT, Latz E, Czura CJ, et al. HMGB1 signals through toll-like receptor (TLR) 4 and TLR2. Shock. 2006; 26:174–9. [PubMed: 16878026]
10. Jiang DH, Liang JR, Fan J, Yu S, Chen SP, Luo Y, et al. Regulation of lung injury and repair by toll-like receptors and hyaluronan. Nat Med. 2005; 11:1173–9. [PubMed: 16244651]
11. Schaefer L, Babelova A, Kiss E, Hausser HJ, Baliova M, Krzyzankova M, et al. The matrix component biglycan is proinflammatory and signals through toll-like receptors 4 and 2 in macrophages. J Clin Invest. 2005; 115:2223–33. [PubMed: 16025156]
12. Quintana FJ, Cohen IR. Heat shock proteins as endogenous adjuvants in sterile and septic inflammation. J Immunol. 2005; 175:2777–82. [PubMed: 16116161]
13. Schroder K, Tschopp J. The inflammasomes. Cell. 2010; 140:821–32. [PubMed: 20303873]
14. Mariathasan S, Weiss DS, Newton K, McBride J, O'Rourke K, Roose-Girma M, et al. Cryopyrin activates the inflammasome in response to toxins and ATP. Nature. 2006; 440:228–32. [PubMed: 16407890]
15. Chakfe Y, Seguin R, Antel JP, Morissette C, Malo D, Henderson D, et al. ADP and AMP induce interleukin-1 beta release from microglial cells through activation of ATP-primed $P2X_7$ receptor channels. J Neurosci. 2002; 22:3061–9. [PubMed: 11943809]
16. Martinon F, Petrilli V, Mayor A, Tardivel A, Tschopp J. Gout-associated uric acid crystals activate the NALP3 inflammasome. Nature. 2006; 440:237–41. [PubMed: 16407889]
17. Martinon F. Mechanisms of uric acid crystal-mediated autoinflammation. Immunol Rev. 2010; 233:218–32. [PubMed: 20193002]
18. Gordon JL. Extracellular ATP - effects, sources and fate. Biochem J. 1986; 233:309–19. [PubMed: 3006665]
19. Iyer SS, Pulskens WP, Sadler JJ, Butter LM, Teske GJ, Ulland TK, et al. Necrotic cells trigger a sterile inflammatory response through the Nlrp3 inflammasome. Proc Natl Acad Sci U S A. 2009; 106:20388–93. [PubMed: 19918053]
20. Gabay C, Lamacchia C, Palmer G. IL-1 pathways in inflammation and human diseases. Nat Rev Rheumatol. 2010; 6:232–41. [PubMed: 20177398]
21. McDonald B, Pittman K, Menezes GB, Hirota SA, Slaba I, Waterhouse CCM, et al. Intravascular danger signals guide neutrophils to sites of sterile inflammation. Science. 2010; 330:362–6. [PubMed: 20947763]
22. Ghiringhelli F, Apetoh L, Tesniere A, Aymeric L, Ma YT, Ortiz C, et al. Activation of the NLRP3 inflammasome in dendritic cells induces IL-1 beta-dependent adaptive immunity against tumors. Nat Med. 2009; 15:1170–9. [PubMed: 19767732]
23. Acosta-Rodriguez EV, Napolitani G, Lanzavecchia A, Sallusto F. Interleukins 1 beta and 6 but not transforming growth factor-beta are essential for the differentiation of interleukin 17- producing human T helper cells. Nat Immunol. 2007; 8:942–9. [PubMed: 17676045]
24. Sironi M, Breviario F, Proserpio P, Biondi A, Vecchi A, Vandamme J, et al. IL-1 stimulates IL-6 production in endothelial cells. J Immunol. 1989; 142:549–53. [PubMed: 2783442]
25. Wesa AK, Galy A. IL-1 beta induces dendritic cells to produce IL-12. Int Immunol. 2001; 13:1053–61. [PubMed: 11470775]

26. Oldenburg SJ, Jackson JB, Westcott SL, Halas NJ. Infrared extinction properties of gold nanoshells. Appl Phys Lett. 1999; 75:2897–9.
27. Brinson BE, Lassiter JB, Levin CS, Bardhan R, Mirin N, Halas NJ. Nanoshells made easy: improving Au layer growth on nanoparticle surfaces. Langmuir. 2008; 24:14166–71. [PubMed: 19360963]
28. Stober W, Fink A, Bohn E. Controlled growth of monodisperse silica spheres in micron size range. J Colloid Interface Sci. 1968; 26:62–9.
29. Duff DG, Baiker A, Edwards PP. A new hydrosol of gold clusters. 1. formation and particle-size variation. Langmuir. 1993; 9:2301–9.
30. Gasse P, Riteau N, Charron S, Girre S, Fick L, Petrilli V, et al. Uric acid is a danger signal activating NALP3 inflammasome in lung injury inflammation and fibrosis. Am J Respir Crit Care Med. 2009; 179:903–13. [PubMed: 19218193]
31. Dulkeith E, Morteani AC, Niedereichholz T, Klar TA, Feldmann J, Levi SA, et al. Fluorescence quenching of dye molecules near gold nanoparticles: radiative and nonradiative effects. Phys Rev Lett. 2002; 89:203002-1–4. [PubMed: 12443474]
32. Crowe WE, Altamirano J, Huerto L, Alvarezleefmans FJ. Volume changes in single N1E-115 neuroblastoma-cells measured with a fluorescent-probe. Neuroscience. 1995; 69:283–6. [PubMed: 8637626]
33. Sonawane ND, Thiagarajah JR, Verkman AS. Chloride concentration in endosomes measured using a ratioable fluorescent Cl^- indicator - evidence for chloride accumulation during acidification. J Biol Chem. 2002; 277:5506–13. [PubMed: 11741919]
34. Roti JLR. Cellular responses to hyperthermia (40–46 degrees C): cell killing and molecular events. Int J Hyperther. 2008; 24:3–15.
35. Zhang HG, Mehta K, Cohen P, Guha C. Hyperthermia on immune regulation: a temperature's story. Cancer Lett. 2008; 271:191–204. [PubMed: 18597930]
36. Pelegrin P, Barroso-Gutierrez C, Surprenant A. $P2X_7$ receptor differentially couples to distinct release pathways for IL-1 β in mouse macrophage. J Immunol. 2008; 180:7147–57. [PubMed: 18490713]
37. Martinon F, Burns K, Tschopp J. The inflammasome: a molecular platform triggering activation of inflammatory caspases and processing of proIL-beta. Mol Cell. 2002; 10:417–26. [PubMed: 12191486]
38. Shi Y, Evans JE, Rock KL. Molecular identification of a danger signal that alerts the immune system to dying cells. Nature. 2003; 425:516–21. [PubMed: 14520412]
39. Shi Y. Caught red-handed: uric acid is an agent of inflammation. J Clin Invest. 2010; 120:1809–11. [PubMed: 20501951]
40. Xie H, Diagaradjane P, Deorukhkar AA, Goins B, Bao A, Phillips WT, et al. Integrin αvβ3-targeted gold nanoshells augment tumor vasculature-specific imaging and therapy. Int J Nanomed. 2011; 6:259–69.
41. Basu S, Binder RJ, Suto R, Anderson KM, Srivastava PK. Necrotic but not apoptotic cell death releases heat shock proteins, which deliver a partial maturation signal to dendritic cells and activate the NF-kappa B pathway. Int Immunol. 2000; 12:1539–46. [PubMed: 11058573]
42. Rovere-Querini P, Capobianco A, Scaffidi P, Valentinis B, Catalanotti F, Giazzon M, et al. HMGB1 is an endogenous immune adjuvant released by necrotic cells. EMBO Reports. 2004; 5:825–30. [PubMed: 15272298]
43. Ghanem G, Loir B, Morandini R, Sales F, Lienard D, Eggermont A, et al. On the release and half-life of S100B protein in the peripheral blood of melanoma patients. Int J Cancer. 2001; 94:586–90. [PubMed: 11745448]
44. Ishii KJ, Suzuki K, Coban C, Takeshita F, Itoh Y, Matoba H, et al. Genomic DNA released by dying cells induces the maturation of APCs. J Immunol. 2001; 167:2602–7. [PubMed: 11509601]
45. Cavassani KA, Ishii M, Wen H, Schaller MA, Lincoln PM, Lukacs NW, et al. TLR3 is an endogenous sensor of tissue necrosis during acute inflammatory events. J Exp Med. 2008; 205:2609–21. [PubMed: 18838547]

46. Vanden Berghe T, Kalai M, Denecker G, Meeus A, Saelens X, Vandenabeele P. Necrosis is associated with IL-6 production but apoptosis is not. Cell Signal. 2006; 18:328–35. [PubMed: 16023831]
47. Lepock JR. Cellular effects of hyperthermia: relevance to the minimum dose for thermal damage. Int J Hyperther. 2003; 19:252–66.
48. Ito A, Honda H, Kobayashi T. Cancer immunotherapy based on intracellular hyperthermia using magnetite nanoparticles: a novel concept of “heat-controlled necrosis” with heat shock protein expression. Cancer Immunol Immunother. 2006; 55:320–8. [PubMed: 16133113]
49. Liu G-J, Moriyasu F, Hirokawa T, Rexiati M, Yamada M, Imai Y. Expression of heat shock protein 70 in rabbit liver after contrast-enhanced ultrasound and radiofrequency ablation. Ultrasound Med Biol. 2010; 36:78–85. [PubMed: 19931970]
50. Brusa D, Migliore E, Garetto S, Simone M, Matera L. Immunogenicity of 56 degrees C and UVC-treated prostate cancer is associated with release of HSP70 and HMGBI from necrotic cells. Prostate. 2009; 69:1343–52. [PubMed: 19496055]
51. Peter C, Wesselborg S, Herrmann M, Lauber K. Dangerous attraction: phagocyte recruitment and danger signals of apoptotic and necrotic cells. Apoptosis. 2010; 15:1007–28. [PubMed: 20157780]
52. Hildebrandt B, Wust P, Ahlers O, Dieing A, Sreenivasa G, Kerner T, et al. The cellular and molecular basis of hyperthermia. Crit Rev Oncol Hematol. 2002; 43:33–56. [PubMed: 12098606]
53. Knudsen S, Schardt A, Buhl T, Boeckmann L, Schon MP, Neumann C, et al. Enhanced T-cell activation by immature dendritic cells loaded with HSP70-expressing heat-killed melanoma cells. Exp Dermatol. 2010; 19:108–16. [PubMed: 19758341]
54. Liu K, Iyoda T, Saternus M, Kimura Y, Inaba K, Steinman RM. Immune tolerance after delivery of dying cells to dendritic cells in situ. J Exp Med. 2002; 196:1091–7. [PubMed: 12391020]

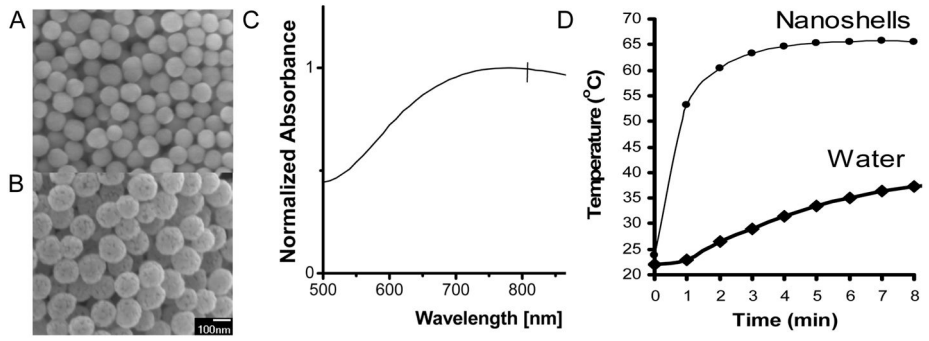

Figure 1.

Characterization of Au nanoshells used in this study. (A) Scanning electron microscopy (SEM) image of synthesized silica nanoparticles 119 ± 11 nm diameter and (B) Au nanoshells. (C) UV-Vis absorption spectra of gold nanoshells in water. The nanoshells have a SPR peak at 780nm. (D) Heating profile of Au nanoshells dispersed in water in the absence of cells.

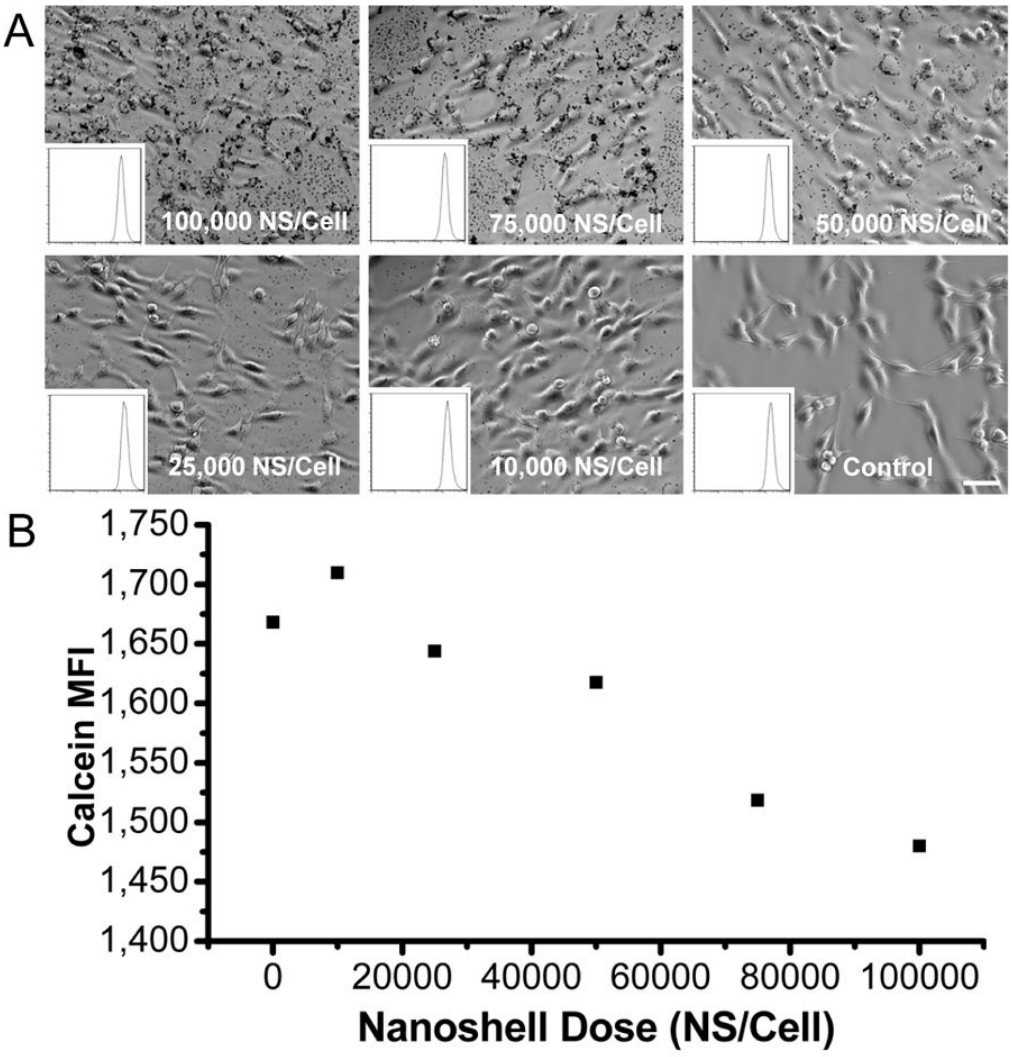

Figure 2.

Cellular uptake of Au nanoshells at different dosage of nanoshells. (A) Light microscopy images of cells incubated with nanoshells from 100,000–10,000 nanoshells/cell. Scale bar = 25μm (B) Geometric mean fluorescence (MFI) of calcein in cells incubated with 200 μg/ml calcein and different dosage of Au nanoshells.

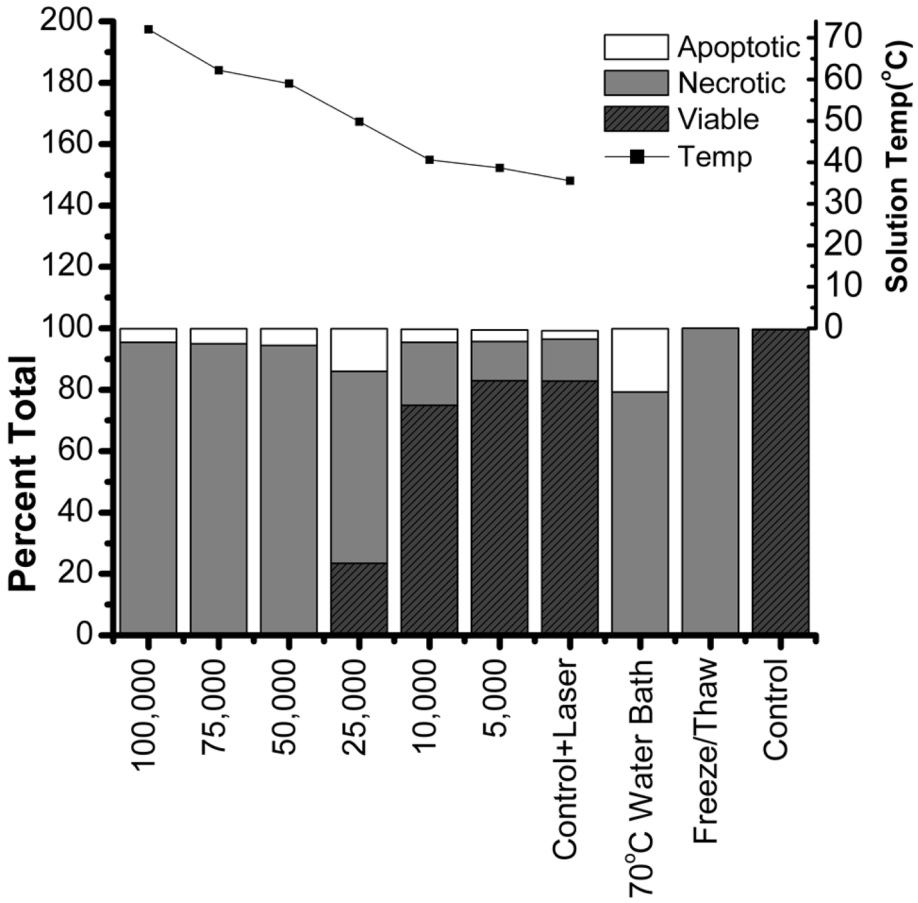

Figure 3.

Mode of cell death and final solution temperature of cell suspension. TC1 cells were incubated with indicated doses of Au nanoshells for 4 h followed by the removal of excess nanoshells. The cells suspended in 100 μl medium were irradiated by a 810 nm laser at 23W/cm^2 for 5 minutes. The solution temperature was measured immediately following the NEPTT. Cell death was evaluated by both Annexin V-FITC and 7-AAD fluorescent staining. Cells incubated in a water bath at 70°C for 5 minutes or exposed to 3 cycles of freeze thaw were used as positive controls for cell death. Cells incubated in cell culture media at 37°C were used as negative controls (Control). Experiments were repeated three times independently.

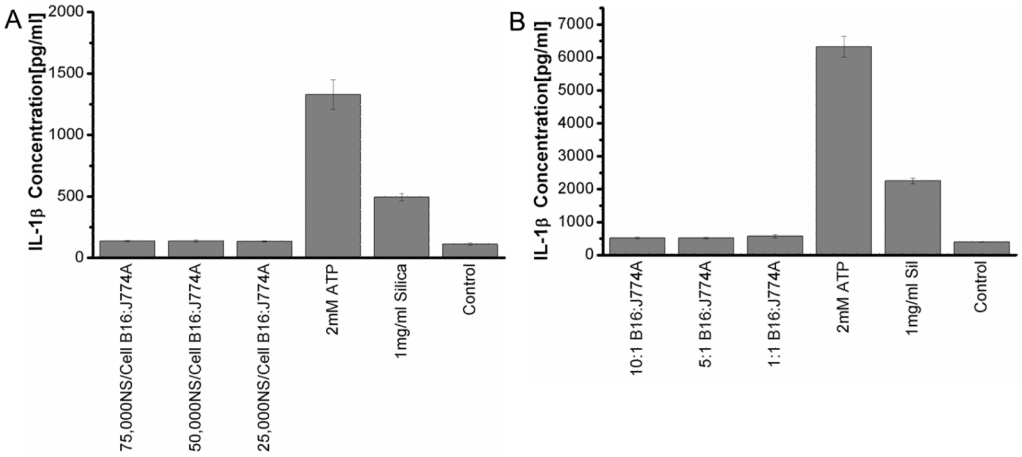

Figure 4.

The stimulation of inflammasomes by NEPTT-treated B16 cells. (A) J774A.1 macrophage cells were stimulated with supernatant fractions collected from treated B16 cells. A ratio of 10:1 of B16 to J774A.1cells was used. (B) J774A.1 macrophage cells were stimulated with supernatant fractions collected from treated B16 cells at ratios from 10:1 to 1:1 for at Au nanoshell dosing of 75,000 nanoshells/cell. IL-1β secreted by stimulated macrophages were collected after 24 h and quantified by ELISA. 2 mM ATP and 1 mg/ml Min-U-Sil 15 silica particles were used as positive controls for inflammasome activation. Untreated cells were used as a negative control (Control). Values are mean ± S.D. Experiments are representative of three independent experiments.

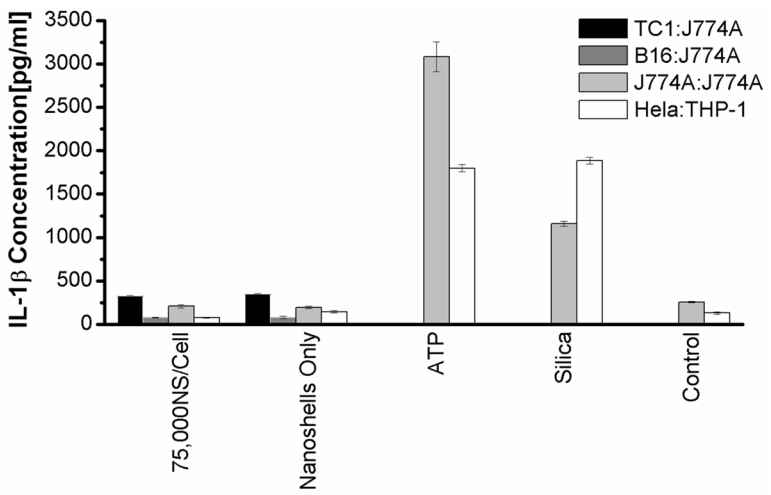

Figure 5.

The stimulation of inflammasomes by different cells treated with NEPTT. Either J774A.1 (dark or grey bars) or THP-1 (White bars) macrophage cells were stimulated with supernatant fractions collected from NEPTT-treated cells. The ratio of NEPTT-treated cells to macrophage was 1:1 and 75,000 nanoshells/cell was used. Three murine cell lines, TC1, B16, and J774A.1 were used to stimulate J774A.1 macrophages, and human Hela cells used to stimulate THP-1 macrophage cells. DPBS treated with NEPTT in the absence of cells was used as a negative control (Media Control). 2 mM ATP and 1 mg/ml Min-U-Sil 15 silica were used as positive controls. IL-1β secreted by macrophages were collected after 24 h and quantified by ELISA. Untreated cells were used as a negative control (Control). Values are mean ± SD. Experiments are representative of three independent experiments.

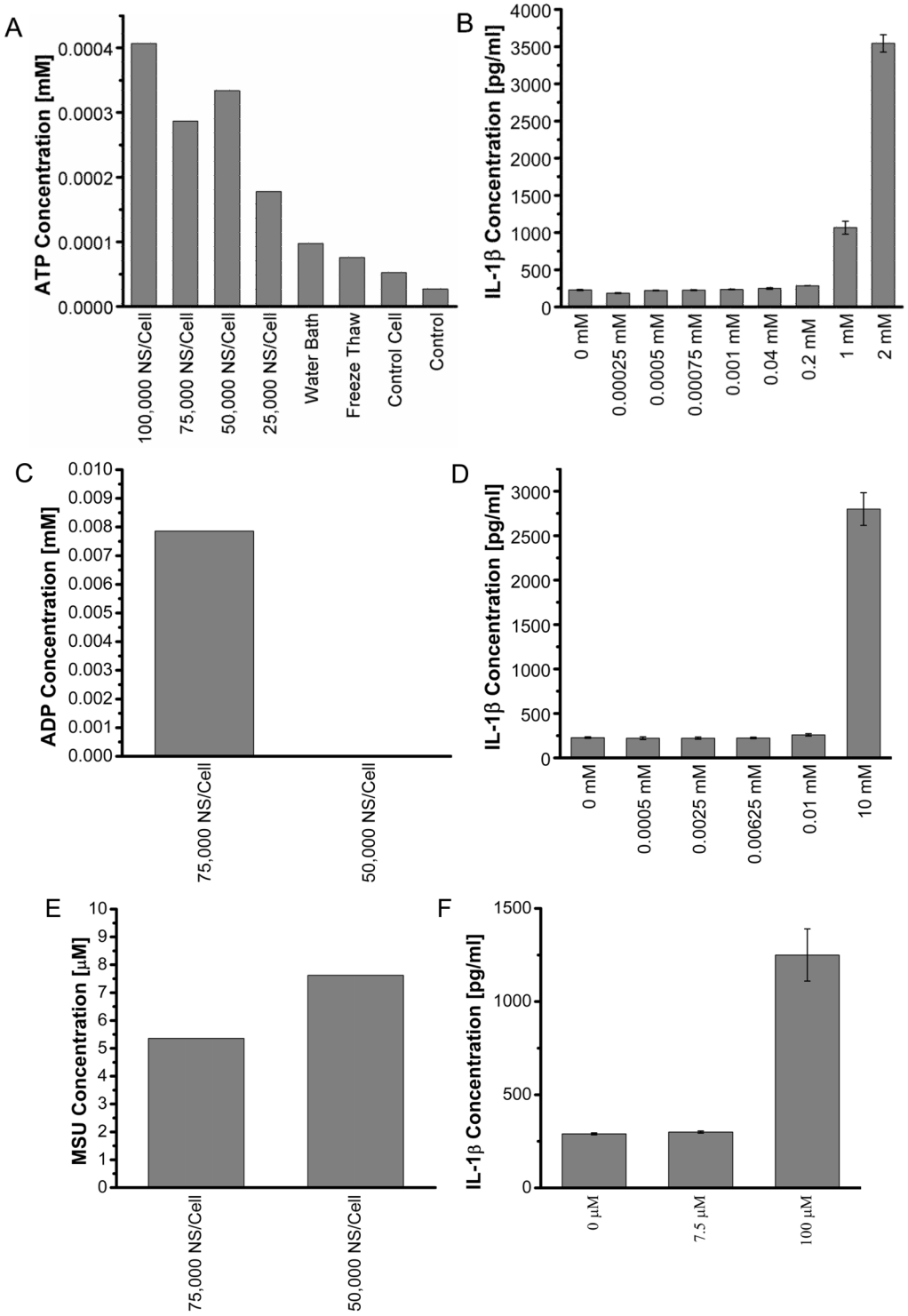

Figure 6.

Quantification of DAMPs released from NEPTT-treated cells and the activation of inflammasomes of each DAMP at different concentrations. (A) Quantification of ATP released from NEPTT-treated at different dosages of nanoshells or controls. Untreated cells were used as a negative control (Control). (B) IL-1β production by J744A.1 stimulated with

standard ATP with the concentration range of 0–2 mM. (C) Quantification of ADP released from NEPTT-treated cells at different dosages of nanoshells. (D) IL-1β production by J744A.1 stimulated with standard ADP with the concentration range of 0–10 mM ADP. (E) Quantification of uric acid released from NEPTT-treated cells at different dosages of nanoshells. (F) IL-1β production by J744A.1 stimulated with standard MSU with the concentration range of 0–100 μM MSU. IL-1β secreted by macrophages were collected after 24 h and quantified by ELISA. Values are mean ± SD. Experiments are representative of three independent experiments.